A CENTROIDAL VORONOI TESSELLATION BASED APPROACH FOR CREATING GRAIN MORPHOLOGY FOR CRYSTAL PLASTICITY FINITE ELEMENT SIMULATIONS

Ling Li[1*], Luming Shen[2], Gwénaëlle Proust[3]

[1] Corresponding author: lili1626@uni.sydney.edu.au
[2] luming.shen@sydney.edu.au
[3] gwenaelle.proust@sydney.edu.au
School of Civil Engineering, The University of Sydney, NSW 2006, Australia

Key Words: *Crystal Plasticity, Microstructure, Centroidal Voronoi Tessellation, Grain Morphology, Finite Element Method.*

Abstract. A simple approach based on centroidal Voronoi tessellation (CVT) is proposed here to create three-dimensional microstructures, for crystal plasticity finite element (CPFE) simulations. In the proposed approach, the grain morphology for any given specimen geometry is created with a predetermined grain size. Instead of using the conventional way that generates the Voronoi cells first and then meshes them into finite elements, this new approach discretises the pre-meshed specimen with the grain seeds generated by the CVT method. This new technique prevents the presence of high density mesh at the vertices of Voronoi cells, and can tessellate arbitrary geometry much more easily. Using a grain aspect scaling algorithm, the proposed approach can create any arbitrary microstructure with a given grain size and aspect ratio. Examples for non-equiaxed polycrystals with different element types are shown. Specimens with irregular shapes and voids are tessellated using this new approach. The grain aspect scaling algorithm is not limited to CVT but can be used with arbitrary grain seeds, offering great flexibility to model diverse material morphologies. It is shown that this proposed approach is simple and efficient.

1 INTRODUCTION

The Voronoi tessellation (VT) method has been extensively used for a host of applications [1]. It divides a given domain into convex polyhedra which can naturally represent individual crystals (grains) in metals. The Voronoi cells (also named Voronoi regions) are generated by the perpendicular bisectors of the lines joining the generators [2]. In the past few decades, people usually employed the VT method to create computational models for finite element and meshfree analysis [3-5]. For instance, Benedetti and Aliabadi [6] modelled intergranular degradation and failure in three-dimensional (3D) polycrystalline microstructures created by VT method using anisotropic elasticity simulations. Recently, the VT method has been incorporated with crystal plasticity finite element (CPFE) simulations to generate artificial grain structure of polycrystals. Its effectiveness and robustness have been verified for CPFE applications in terms of nanoindentation, fatigue, grain size and grain boundary effects, and twinning [7-12]. Furthermore, Abdolvand and Daymond [13] studied the effects of grain boundary geometry and texture on twin inception and propagation. Their CPFE simulations captured the main feature of the average behaviour of twins observed experimentally.

In general, the position of the Voronoi generator (also called generating point or seed) does

not coincide with the mass centroid of the Voronoi cell. The centroidal Voronoi tessellation (CVT) is a particular case for which the generators are the same points as the mass centroids of the corresponding Voronoi cells. Studies have shown that CVTs often provide optimal point distributions, thus making CVTs based mesh generation and optimization techniques very effective [14]. CVT is an optimised solution for simulating equiaxed grains, due to the fact that it uses perpendicular bisectors and can minimise the energy (also named error or cost) function. Hence it will generate a more stable microstructure with a lower system energy. There are several algorithms for determining CVTs, for instance, the MacQueen's method [15] and the Lloyd's method [16] are two classic theories among them. Based on these two methods, a probabilistic Lloyd's method was proposed by Du et al. [4, 17], which is efficient and does not require the construction of the Voronoi cells until the final step. However, convergence with this method is difficult to achieve, since the energy function tends to be trapped at local minima. Very recently, Jie et al. [18] have significantly improved its convergence performance by introducing the simulated annealing concept.

Some existing packages provide professional solutions to the Voronoi tessellation in both 2D and 3D, such as Voro++ [19], Qhull [20] and Neper [21]. Additionally, Zhang et al. [22, 23] developed a 3D controlled Poisson Voronoi tessellation (CPVT) model for generating polycrystalline grain structures for micromechanics simulations. The CPVT model can create random to uniform grain structures, and produce equivalent characteristics to the actual grain structure, such as the mean grain size and the grain size distribution. In spite of these existing approaches being effective and robust, they can only create equiaxed Voronoi cells. This is due to the nature of the perpendicular bisecting algorithm. For a scenario in which the grains are non-equiaxed, e.g. elongated grains, and the specimen domain is not a box, it is fairly difficult to generate the correct grain structure. For simple geometry, such as a box, one can create and tessellate the brick domain and then scale with the grain aspect ratio. However, for spheres, rings, springs, round corners, and voids, the existing methods show their limitations. Another problem regarding FE model generation is the mesh singularity at the vertices of Voronoi cells. During the procedure of meshing Voronoi cells into finite elements, it is most likely that it will be necessary to refine the mesh at the vertices in order to get a decent quality. Although Quey et al. [21] and Qian et al. [24] have proposed different solutions to this issue, it is still not fully addressed especially when the geometry is complex.

In the present work, we propose a novel approach to generate grain structures with arbitrary specimen shape and grain aspect ratio for CPFE simulations. Instead of following the conventional routine that is to create the Voronoi generators first and then construct Voronoi cells and finally mesh them into FE models, the new approach meshes the target domain first using finite elements, and then categorises these elements into individual Voronoi aggregates, without generating cell boundaries and dealing with vertices of cells.

2 SCHEME OF THE CVT BASED APPROACH

2.1 Centroidal Voronoi tessellation

Consider a domain $\boldsymbol{\Omega} \subset \mathbb{R}^d$, $d = 2, 3$ tessellated by a set of generators $\{\boldsymbol{g}_i\}_{i=1}^N$ with $\{V_i\}_{i=1}^N$ being the corresponding Voronoi cells. The $\{V_i\}_{i=1}^N$ can be constructed through the VT method [14] as follows:

$$V_i = \left\{ \boldsymbol{x} \in \boldsymbol{\Omega} \mid \|\boldsymbol{x} - \boldsymbol{g}_i\| < \|\boldsymbol{x} - \boldsymbol{g}_j\| \right\}, \ for \ j = 1, \ldots, N, i = 1, \ldots, N, j \neq i \qquad (1)$$

where $\|\cdot\|$ denotes the Euclidean L^2 norm and N is the number of Voronoi generators. Therefore there will be no intersection between two adjacent Voronoi cells except the shared boundary surface or line, and the whole domain $\boldsymbol{\Omega}$ is discretised by all the Voronoi cells, thus

$$V_i \bigcap V_j = \varnothing \; for \; i \neq j$$

$$\bigcup_{i=1}^{N} V_i = \boldsymbol{\Omega} \tag{2}$$

Normally the mass centroids of the Voronoi cells $\{\boldsymbol{c}_i\}_{i=1}^{N}$ are of different positions as the generators. Assuming that the mass density of the domain is $\rho(\boldsymbol{x})$, $\{\boldsymbol{c}_i\}_{i=1}^{N}$ can be calculated as:

$$\boldsymbol{c}_i = \frac{1}{|V_i|}\int_{V_i} \boldsymbol{x}\rho(\boldsymbol{x})d\boldsymbol{x}, \; for \; i=1,\dots,N \tag{3}$$

As aforementioned, CVT is the particular case where $\{\boldsymbol{c}_i\}_{i=1}^{N}$ coincide with $\{\boldsymbol{g}_i\}_{i=1}^{N}$, which leads to a more stable geometry with a minimum level of the energy function E:

$$E(\{\boldsymbol{g}_i\}_{i=1}^{N}, \{V_i\}_{i=1}^{N}) = \sum_{i=1}^{N}\int_{V_i} \|\boldsymbol{x} - \boldsymbol{g}_i\|^2 \rho(\boldsymbol{x})d\boldsymbol{x} \tag{4}$$

For the reason that the CVT can generate more regular Voronoi cells, it is adopted to explicitly obtain a desired grain size. The sizes of centroidal Voronoi cells are very close and predictable compared with the case of randomly generated. In the present work, a code library of CVT based on the probabilistic Lloyd's method [25] is incorporated to produce the CVT generators (see [4, 17, 25] for more details). Since the mass densities in most CP simulations are uniform, $\rho(\boldsymbol{x}) \equiv 1$ is used in the following sections.

2.2 Grain aspect scaling algorithm and element categorisation

Due to the perpendicularly bisecting algorithm of the Voronoi tessellation, the aspect ratio of constructed Voronoi cells tends to be equiaxial. Even though one can scale the generators to distribute as the desired aspect ratio, the Voronoi cells will not be in the desired aspect ratio after tessellation, nor the FE aggregates meshed on each cell. Therefore, instead of using the conventional routine that generates the Voronoi cells first and then meshes them into elements, we change the order of the procedure and apply a grain aspect scaling algorithm to categorise the FE aggregates. As a result, the new approach can create any grain structure with arbitrary grain aspect ratio (in terms of Cartesian coordinates) and can avoid the complex work involved in Voronoi cells construction and meshing. The realisation of the approach is explained in this section.
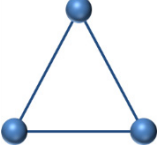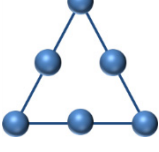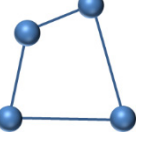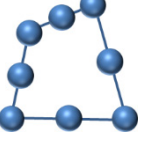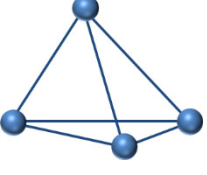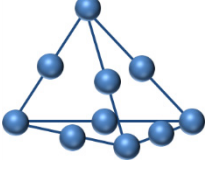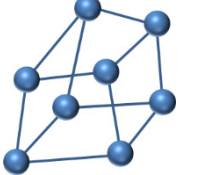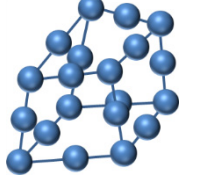
At the first step, the specimen geometry is created and meshed in the framework of FE method, for instance, using commercial software ABAQUS [26]. Nowadays, most of the FE software are highly mature and intelligent, thus people can easily obtain a desired mesh. The meshing is controlled by the FE criteria and in some cases, can be automatic even for complex geometries. Hence, meshing on the whole specimen is more convenient and efficient than meshing the Voronoi cells. In addition, it can be easily proven from [27] that given a uniform mass density $\rho(\boldsymbol{x}) = 1$, the mass centroids $\boldsymbol{c}^e$ of the commonly used element types as listed in

3

table 1 coincide with the coordinates of the node centres:

$$c^e = \frac{1}{n} \sum_{j=1}^{n} x_j^e \qquad (5)$$

where n is the number of nodes of an element and x_j^e the coordinates of each node.

Table 1. The commonly used element types in finite element simulations.

2D	3-node triangle	6-node triangle	4-node quadrilateral	8-node quadrilateral
3D	4-node tetrahedron	10-node tetrahedron	8-node hexahedron	20-node hexahedron

Next, the centroids c^e are used to categorise FE aggregates which represent individual grains. Based on the VT algorithm, if the closest Voronoi generator to an element's c_k^e is g_i, then element k will be categorised to Voronoi cell i and assigned the corresponding crystalline properties for the CPFE simulation. The main idea of the grain aspect scaling algorithm for arbitrary grain shape is that it scales the FE model by given grain aspect ratio, then categorises elements into polycrystalline aggregates, and finally scales the FE model back to the original coordinates. Specifically, the grain aspect ratio is applied to scale the centroids of elements' c^e through dividing by the grain aspect ratio in each direction.

$$\tilde{c}_d^e = \frac{1}{r_d} c_d^e \, , d = 1, 2, 3 \qquad (6)$$

where $\tilde{c}_d^e$ is the scaled centroid of each element, and r_d the value of the grain aspect ratio $r = [r_1, r_2, r_3]$ in direction d, where $\min\{r_1, r_2, r_3\} = 1$. Noted that the summation convention does not apply in the present work. After scaling by the grain aspect ratio, the scaled domain of the FE model becomes

$$\tilde{\Omega}_d^e = \frac{1}{r_d} \Omega_d^e = \frac{1}{r_d} [\max(x_d^e) - \min(x_d^e)], \ d = 1, 2, 3 \qquad (7)$$

Now we can tessellate the scaled domain $\tilde{\boldsymbol{\Omega}}^e$ with a set of CVT generators $\tilde{g}_i$. The number of generators, NP, is determined by the volumes of the domain $\tilde{\boldsymbol{\Omega}}^e$ and the individual grains.

$$\tilde{g}_i \in \tilde{\boldsymbol{\Omega}}^e \, , \ i = 1, \ldots, NP, \ NP = \mathrm{int}(Vol_{\tilde{\Omega}^e} / Vol_{grain}) \qquad (8)$$

4

Using the VT algorithm, we can categorise all the elements $\{e_k\}_{k=1}^{NE}$ (NE is the number of elements) to their corresponding Voronoi cells $\{\tilde{V}_i\}_{i=1}^{NP}$.

$$\tilde{V}_i = \left\{ e_k \mid \left\| \tilde{\boldsymbol{c}}_k^e - \tilde{\boldsymbol{g}}_i \right\| < \left\| \tilde{\boldsymbol{c}}_k^e - \tilde{\boldsymbol{g}}_j \right\| \right\}, \ for \ i=1,...,NP, \ j=1,...,NP, \ j \neq i, \ k=1,...,NE \qquad (9)$$

After the categorisation, the grain aspect ratio $\tilde{r}_d$ of $\{\tilde{V}_i\}_{i=1}^{NP}$ is determined by the uniform distribution of CVT generators, i.e. $\tilde{r}_d = 1$. Therefore, this step produces equiaxed grains similarly as conventional approaches do.

The final step is to scale the FE model back to the original coordinates, by multiplying the grain aspect ratio by $\{\tilde{V}_i\}_{i=1}^{NP}$. Hence, the finial grain aspect ratio of the grain structure r_d^e is:

$$r_d^e = \tilde{r}_d r_d = r_d \ , d = 1,2,3 \qquad (10)$$

As a result, the scaling algorithm guarantees that the initial model has not been changed in term of geometry while possessing the desired grain aspect ratio r_d. In practice, since the coordinates of the FE model do not change, step (10) can be simply skipped by using the initial coordinates and updating the information of crystalline categorisation before starting the CPFE simulation.

3 EXAMPLES OF ARBITRARY SHAPE AND GRAIN SIZE SPECIMEN

During the categorisation procedure, crystalline properties are assigned to individual grains according to CPFE framework. The new approach by categorising the pre-meshed FE model to individual grains offers great flexibility to model the specimen shape and grain aspect ratio. Furthermore, regardless of what element type is used, the approach will generate similar grain structures for a same set of Voronoi generators. Fig. 1 shows a polycrystalline cylinder that was tessellated using tetrahedral and hexahedral elements, respectively. Each colour of the FE aggregates represents a specific crystallographic orientation. The dimension of the cylinder is $1000 \times 1000 \times 2000$ μm³ (X×Y×Z) with a given grain size of $150 \times 150 \times 450$ μm³ (X×Y×Z). The specimen was meshed into 560,411 tetrahedral elements and 247,200 hexahedral elements, respectively. As can be seen from Fig. 1, using the same set of Voronoi generators, the grain structures of the CPFE model are very similar except for the grain boundary regions; this difference is caused by different element types. It is shown in Fig. 1 that the proposed approach can reach a desired grain size and handle the grain aspect ratio very well. Nonetheless, it is hard to conclude which element type is better for the approach since the grain boundary is arbitrary. As highlighted in Fig. 1, some grain boundaries are jagged using tetrahedral elements whereas they are straight using hexahedral elements, and vice versa. The jagged grain boundaries are an inherent drawback since the mesh is pre-determined; however, this weakness can be neglected if the element is relatively small compared with the grain size.

Since the specimen is created and meshed in FE framework, the intrinsic difficulty of VT method in terms of tessellating concaved domain is completely addressed. Therefore the new approach can easily generate polycrystalline structures with concaved surfaces and voids. The flexibility of tessellating complex specimen shape is demonstrated in Fig. 2. A half sphere with a radius of 500 μm as shown in Fig. 2(a) has a spherical void with a radius of 300 μm. The model contains 269,740 hexahedral elements and the grain size is $80 \times 160 \times 40$ μm³ (X×Y×Z). Again, this example shows the capability of dealing with any grain aspect ratio.

5

Furthermore, an even more complex specimen, a half circular tube, is shown in Fig. 2(b). The inner radius of the cross section is 300 μm and the outer radius is 500 μm. It contains 196,416 hexahedral elements and the grain size is $200\times200\times200$ μm^3 (X×Y×Z). It is clearly shown in Fig. 2(b) that the grains follow the CVT pattern, which is regular and equiaxed.
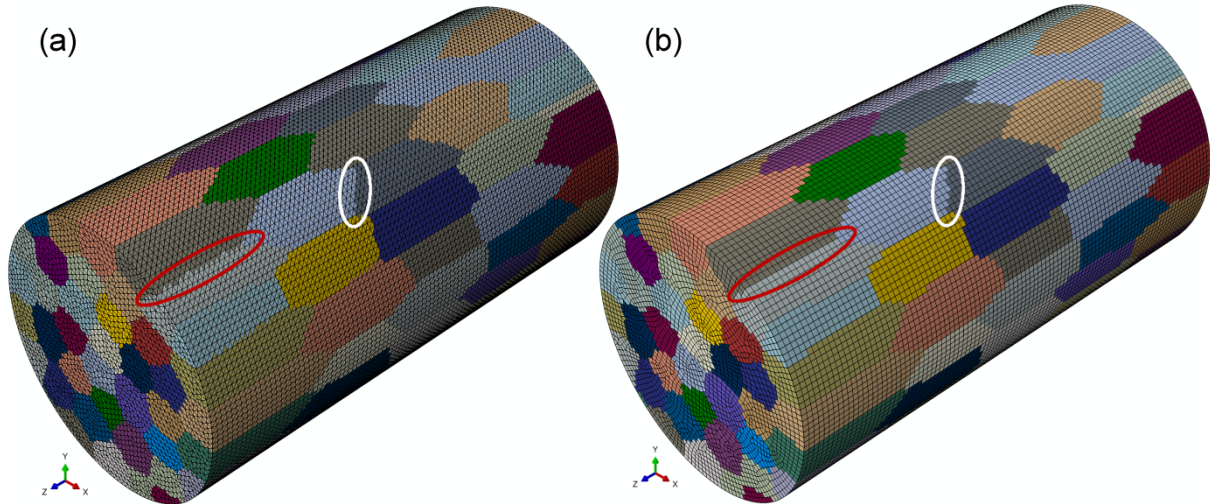

Figure 1: Discretisations of a polycrystalline cylinder with a given grain size of $150\times150\times450$ μm3 (X×Y×Z) using (a) tetrahedral and (b) hexahedral finite elements. Each colour represents a specific crystallographic orientation.

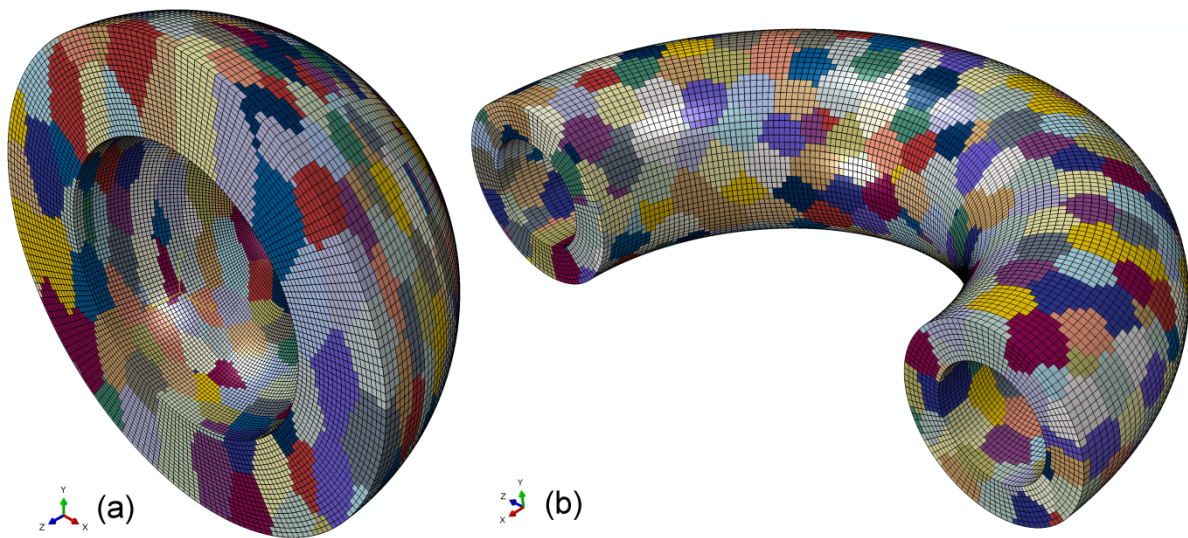
Figure 2: Discretisations of (a) a central-voided polycrystalline half sphere with a given grain size of $80\times160\times40$ μm^3 (X×Y×Z) and (b) a polycrystalline half circular tube with a given grain size of $200\times200\times200$ μm^3 (X×Y×Z). Each colour represents a specific crystallographic orientation.

4 CONCLUSION

A new approach for creating polycrystalline microstructures for CPFE simulations is developed based on the CVT method. Instead of using the conventional routine that tessellates specimen geometry first and then mesh the Voronoi cells, the new approach meshes specimen geometry into finite elements in the first place, and then categorises them into FE aggregates

through a grain aspect scaling algorithm. During the categorisation procedure, crystalline properties are assigned to individual grains before the CPFE simulation. Therefore, there is no need to construct the Voronoi cells and mesh each cell, which avoids a vast amount of calculation. It is found that most of the computing time of the new approach is spent on producing the centroidal Voronoi generators, while the specimen meshing and element categorisation only occupy a small portion of the total time. This is a great improvement of efficiency compared with conventional methods that construct and mesh each Voronoi cells.

The approach can deal with concave or voided geometries without difficulty and completely avoids mesh refinement at the vertices of the Voronoi cells. More importantly, it can generate grain structures with arbitrary grain aspect ratio, providing great flexibility in simulating various material morphologies. Examples are shown by tessellating specimens which contain irregular shapes and voids with different element types and grain aspect ratios. Although the CVT is employed to explicitly obtain a desired grain size, this does not mean that the new approach is limited to CVT. As a matter of fact, the Voronoi generators can be arbitrary points, as long as they are consistent with the physical implications of the crystalline microstructure. The required input information for the new approach is only the specimen geometry, and grain size and shape.

ACKNOWLEDGEMENTS

REFERRENCES

[1] A. Okabe, B. Boots, K. Sugihara, S.N. Chiu, Spatial tessellations: concepts and applications of Voronoi diagrams, Wiley. com, 2009.

[2] S. Kumar, S.K. Kurtz, Simulation of material microstructure using a 3D voronoi tesselation: Calculation of effective thermal expansion coefficient of polycrystalline materials, Acta Metall. 42 (1994) 3917-3927.

[3] J. Ruppert, A Delaunay refinement algorithm for quality 2-dimensional mesh generation, J. Algorithm. 18 (1995) 548-585.

[4] Q. Du, M. Gunzburger, L. Ju, Meshfree, probabilistic determination of point sets and support regions for meshless computing, Comput. Method. Appl. M 191 (2002) 1349-1366.

[5] F. Fritzen, T. Böhlke, E. Schnack, Periodic three-dimensional mesh generation for crystalline aggregates based on Voronoi tessellations, Comput. Mech. 43 (2009) 701-713.

[6] I. Benedetti, M.H. Aliabadi, A three-dimensional cohesive-frictional grain-boundary micromechanical model for intergranular degradation and failure in polycrystalline materials, Comput. Method. Appl. M 265 (2013) 36-62.

[7] W. Li, N. Zabaras, A virtual environment for the interrogation of 3D polycrystalline microstructures including grain size effects, Comp. Mater. Sci. 44 (2009) 1163-1177.

[8] L. Li, L. Shen, G. Proust, C.K.S. Moy, G. Ranzi, Three-dimensional crystal plasticity finite element simulation of nanoindentation on aluminium alloy 2024, Mater. Sci. Eng. A 579 (2013) 41-49.

[9] Y. Li, L. Zhu, Y. Liu, Y. Wei, Y. Wu, D. Tang, Z. Mi, On the strain hardening and texture evolution in high manganese steels: Experiments and numerical investigation, J. Mech. Phys. Solids. 61 (2013) 2588-2604.

[10] S. El Shawish, L. Cizelj, I. Simonovski, Modeling grain boundaries in polycrystals using cohesive elements: Qualitative and quantitative analysis, Nucl. Eng. Des. 261 (2013) 371-381.

[11] L. Li, L. Shen, G. Proust, Crystal plasticity finite element simulations of polycrystalline aluminium alloy under cyclic loading, Adv. Mater. Res. 891-892 (2014) 1609-1614.

[12] N. Salajegheh, D.L. McDowell, Microstructure-sensitive weighted probability approach for modeling surface to bulk transition of high cycle fatigue failures dominated by primary inclusions, Int. J. Fatigue. 59 (2014) 188-199.

[13] H. Abdolvand, M.R. Daymond, Multi-scale modeling and experimental study of twin inception and propagation in hexagonal close-packed materials using a crystal plasticity finite element approach—Part I: Average behavior, J. Mech. Phys. Solids. 61 (2013) 783-802.

[14] Q. Du, M. Gunzburger, Grid generation and optimization based on centroidal Voronoi tessellations, Appl. Math. Comput. 133 (2002) 591-607.

[15] J. MacQueen, Some methods for classification and analysis of multivariate observations, in: Proceedings of the fifth Berkeley symposium on mathematical statistics and probability, California, USA, 1967, pp. 14.

[16] S.P. Lloyd, Least-squares quantization in PCM, IEEE. T. Inform. Theory 28 (1982) 129-137.

[17] L. Ju, Q. Du, M. Gunzburger, Probabilistic methods for centroidal Voronoi tessellations and their parallel implementations, Parallel. Comput. 28 (2002) 1477-1500.

[18] Y.-x. Jie, X.-d. Fu, Y. Liu, Mesh generation for FEM based on centroidal Voronoi tessellations, Math. Comput. Simulat. 97 (2014) 68-79.

[19] C.H. Rycroft, VORO++: A three-dimensional Voronoi cell library in C++, Chaos: An Interdisciplinary Journal of Nonlinear Science 19 (2009) -.

[20] B. Barber, H. Huhdanpaa, Qhull manual, The Geometry Center, Minneapolis MN (2003).

[21] R. Quey, P. Dawson, F. Barbe, Large-scale 3D random polycrystals for the finite element method: Generation, meshing and remeshing, Comput. Method. Appl. M 200 (2011) 1729-1745.

[22] P. Zhang, D. Balint, J. Lin, An integrated scheme for crystal plasticity analysis: Virtual grain structure generation, Comp. Mater. Sci. 50 (2011) 2854-2864.

[23] P. Zhang, M. Karimpour, D. Balint, J. Lin, Three-dimensional virtual grain structure generation with grain size control, Mech. Mater. 55 (2012) 89-101.

[24] J. Qian, Y. Zhang, W. Wang, A.C. Lewis, M.A.S. Qidwai, A.B. Geltmacher, Quality improvement of non-manifold hexahedral meshes for critical feature determination of microstructure materials, Int. J. Numer. Meth. Eng 82 (2010) 1406-1423.

[25] J. Burkardt, M. Gunzburger, J. Peterson, R. Brannon, User manual and supporting information for library of codes for centroidal Voronoi point placement and associated zeroth, first, and second moment determination, SAND Report SAND2002-0099, Sandia National Laboratories, Albuquerque (2002).

[26] ABAQUS User's Manual, Version 6.10, Hibbit, Karlsson and Sorensen Inc. (2011).

[27] M.F. Mammana, B. Micale, M. Pennisi, On the centroids of polygons and polyhedra, in: Forum Geometricorum, 2008, pp. 121-130.